THE COMMISSIONING STATUS OF RHIC*

M. Harrison#, BNL, Upton, NY

Abstract

The construction and commissioning status of the Relativistic Heavy Ion Collider, RHIC, is discussed. Those novel features of a heavy ion Collider that are distinct from conventional hadron Colliders in general are noted. These features are derived from the experimental requirements of operation with a variety of ion species over a wide energy range including collisions between ions of unequal energies. The paper notes other challenging issues for the Collider including intrabeam scattering, interaction-region error compensation, magnet alignments, and matched transition-energy jump. The project is in the final few months of a seven-year construction cycle and is entering the commissioning phase. A review of the superconducting magnet program is given together with the status of the machine construction and commissioning.

1 INTRODUCTION

The primary motivation for colliding heavy ions at ultra-relativistic energies is the belief that it is possible to create macroscopic volumes of nuclear matter at such extreme conditions of temperature and energy density that a phase transition will occur from hadronic matter to a confined plasma of quarks and gluons. The main goal of the Relativistic Heavy Ion Collider (RHIC is to provide head-on collisions at energies up to 100 GeV/u per beam for very heavy ions, which are defined to be gold $^{197}Au^{79+}$, but the program also calls for lighter ions all the way down to protons and polarized protons. Luminosity requirements for the heaviest ions are specified to be in the $10^{26\text{-}27}$ $cm^{-2} s^{-1}$ range. The higher Au-Au total cross section results in interaction rates comparable to p-p Colliders although this luminosity is several orders of magnitude lower than those machines. A short interaction point (IP) length (<20 cm rms.) is desirable for optimum detector design. The final, though most influential, experiment requirement has been the need for collisions of different ion species (most notably p-Au) at the same center of mass energies per nucleon. This necessitates accommodating mass-to-charge ratios (A/Z) in the range of 1 (p) to 2.5 (Au). Stabilizing the collision point involves equalizing the rotation frequencies of the two beams, which also requires the two rings to operate at different magnetic fields. The complications in the interaction region (IR) where the beams must pass through common magnets dictate a lattice design different from conventional hadron Colliders.

Based on these general requirements, the detailed RHIC machine parameters were derived and are outlined in Table 1. Operation of the RHIC Collider at relatively low energies together with the enhanced intrabeam scattering (IBS), which scales as Z^4/A^2, results in beams of large transverse and longitudinal dimensions. This in turn has ramifications for the lattice (short cells, strong focusing) and magnet aperture. This consideration and the short IP length also determine the rf system requirements. Colliders, unlike fixed target machines, are designed to operate for extended periods at high energies. The economics of power consumption argue strongly for superconducting magnets. RHIC is such a superconducting machine.

Table 1: Major Parameters for the Collider

Kinetic Energy, Inj.-Top, Au	10.8-100	GeV/u
(each beam), protons	28.3-250	GeV
No. of bunches/ring	60	
Circumference	3833.845	m
Number of crossing points	6	
β^*, injection, H/V	10	m
β^*, low-beta insertion, H/V	1	m
Betatron tunes, H/V	28.18/29.18	
Magnetic rigidity, injection	97.5	T-m
top energy	839.5	T-m
Number of dipoles (192/ring + 12 common)	396	
Number of quadrupoles (276 arc + 216 insertion)	492	
Dipole field at 100 GeV/u,Au	3.45	T
Arc dipole effective length	9.45	m
Arc quadrupole gradient	71.2	T-m

2 MACHINE DESIGN AND LAYOUT

The complete RHIC facility is a complex set of accelerators interconnected by beam transfer lines. The collider, shown schematically in Fig. 1, is located in the existing 3.8 km tunnel north of the AGS.

* Work performed under the auspices of the U.S. Department of Energy.
# harrison@bnl.gov

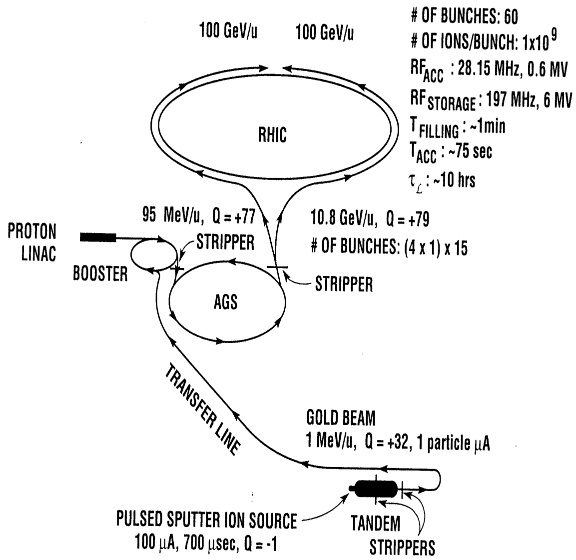

Figure 1: The RHIC Complex

It is comprised of two identical, quasi-circular rings separated horizontally by 90 cm, and oriented to intersect with one another at six locations. Having a 3-fold symmetry, each ring consists of three inner and three outer arcs and six insertion regions joining them. Each arc consists of 11 FODO cells, with each half-cell consisting of a single dipole and a spool-piece assembly containing a quadrupole, sextupole, and concentric correction elements. Fig. 2. shows the Collider layout together with the standard cell schematic.

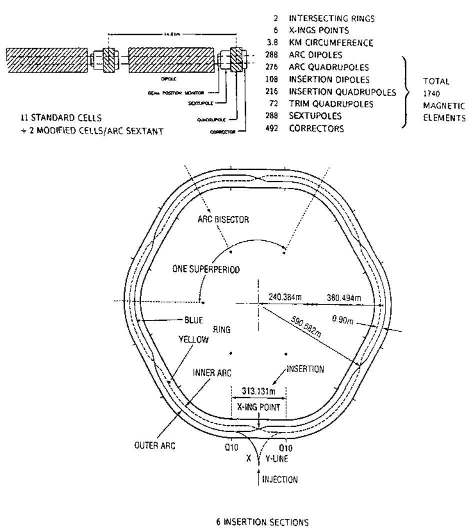

Figure 2: Collider layout and standard cell

The nominal design magnetic rigidity of the dipoles is 840 T-m which corresponds to a design field of 3.45 T at 100 GeV/u. Injection takes place at 97.5 T-m. The half-cell length of 15 m has beta-functions in the range from 10.5 m to 50 m, and a dispersion from 0.8 m to 1.8 m. These relatively small values are dictated by the need to minimize the physical size of a beam (i.e. maximize dynamic aperture and thus intensity lifetime) with relatively large emittances (40πmm-mr normalized 95% transverse, 1.2 eV-s/u longitudinal). The dipole coil inner diameter (i.d.) of 8 cm is determined both by the beam size at injection and by the projected emittance growth which occurs during a store at the lowest collision energy of 30 GeV/u. The quadrupoles, also having a coil i.d. of 8 cm, operate at a maximum gradient of 72 T/m. A cross-section of a dipole of length 9.45 m is shown in Fig 3. The magnets are conceptually similar to the HERA dipoles with a "cold-iron" design and cryogenic transfer lines located in the cryostat.

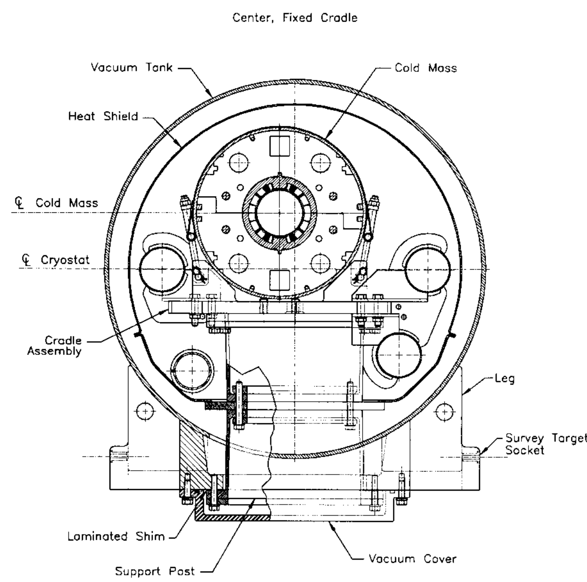

Figure 3: RHIC dipole cross section

Collisions of the beams take place at the crossing point of the insertions. These regions contain the optics necessary for producing small betatron amplitude functions β^*, a zero dispersion at the crossing point, and the magnet steering to bring the beams into head-on collisions. The "non-arc" regions also contain the only warm regions of the machine where the machine utilities reside such as injection, beam abort, rf station, collimators, and specialized instrumentation. Locations available for these devices are the 30 m section between Q3 and Q4, the missing dipole between Q7 and Q8, and the section adjacent to the short D9 dipole. The magnetic elements in the region from Q10 to Q4 are identical in cross-section but different in length to those in the standard cell. The final focus triplet (Q1, Q2, and Q3), and bending magnets (D0 and DX) are non-standard magnets with apertures of 13 cm, 10 cm, and 18 cm, respectively. The focusing is relaxed at injection with a β^*value of 10 m. During collisions at top energy, a β^* of 1 m can be attained resulting a maximum β of about 1400 m in the triplet quadrupoles. The maximum focusing strength of 48 T/m is determined by both the physical beam size in the triplet and the strength of the trim quadrupoles at Q4, Q5, and Q6. The lattice functions in the IR's are shown in Fig. 4. Each insertion is independently adjustable and can be matched over a machine tune range of ±1 unit. The phase advance across the insertion is almost constant during the squeeze, as is the triplet excitation.

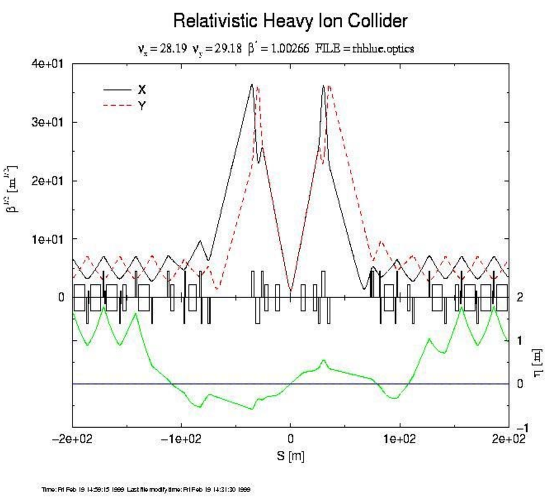

Figure 4: Lattice functions in the interaction regions

3 DESIGN FEATURES

3.1 Unequal Energies

Probing the dynamics of a quark-gluon plasma benefits greatly by the ability to varying the initial conditions which in the context of RHIC means collisions between unequal particle species and energies in addition to merely varying species and collision energy. This requirement precluded a common final focus and the RHIC beams are separated before the final focus. The quadrupole triplet is thus moved further away from the interaction point impacting the aperture requirements. The closest magnet to the interaction point is a large aperture (18cm) dipole operating at 4T. Particle trajectories vary considerably in this magnet.

3.2 Intrabeam Scattering (IBS)

Emittance growth caused by intrabeam scattering [1] is of concern during both injection and storage of the heavy ion beams. At injection, the IBS longitudinal growth time is only 3 minutes. Injection needs to be accomplished in 60s to avoid difficulty in transition crossing and rf rebucketting due to increased longitudinal beam size. At storage, emittance growth occurs in both transverse and longitudinal planes with transverse emittances growing from the initial 10π mm-mr to more than 40π mm-mr during the first several hours of a store. Longitudinal bunch area exceeds the bucket area of 1.2 eV-s/u in about an hour. Collimation systems are designed to intercept particles escaped from the rf buckets. Increasing peak rf voltage only modestly improves the luminosity performance, since transverse growth is so significant. The ultimate improvement can be made if cooling methods are adopted. Maximizing machine performance with large emittance beams required an unusually short cell length to minimize the physical beam size in the arcs.

3.3 IR Error Compensation

In order to maximize the instantaneous luminosity the final focus triplets are designed to enable the collision β^* to be reduced to 1m. Dipoles and triplets of quadrupoles of large bore are placed on both sides of the IP. The $\beta_{\mu\alpha\xi}$ of 1400m, along with the strong IBS growth, results in the 5σ beam size increasing from 35% to about 70% of the triplet magnet coil radius. In order to optimize the field quality in these elements, sophisticated compensation techniques have been developed [2] including individual error correction with tuning shims, amplitude dependent body-ends compensation, low β magnet sorting, and lumped triplet multi-layer corrector packages.

3.4 Transition Crossing

RHIC will be the first superconducting accelerator to cross transition energy. Due to the slow ramping rate of the superconducting magnets, both chromatic nonlinear effects and beam self-field effects are strong at crossing. In addition the superconducting machine environment makes operation vulnerable to magnet quenching arising from beam losses should they occur. A “matched first order” transition jump scheme has been implemented [3] to effectively increase the crossing rate by a factor of 8 during the 60 ms time around transition. With such a scheme the longitudinal emittance growth can be limited to less than 20% at transition while keeping the beam spot size constant to avoid particle losses.

4 SUPERCONDUCTING MAGNET PROGRAM

The Superconducting magnet program for the Project is now complete with the last magnet delivered to the ring in November 1998. The ring magnets naturally fall into two types; the 8cm elements which are used throughout the arc regions and constitute the majority of the magnets, and the smaller number of variable aperture magnets used in the immediate vicinity of the IP. A list of the various magnet types is given in Table 2.

Table 2: RHIC Superconducting Magnet Inventory

8 cm dipoles	360
8 cm quadrupoles	420
IR trim quadrupoles	72
sextupoles	288
8 cm multilayer correctors	420
13 cm IR final focus quadrupoles	72
13 cm IR correctors	72
10 cm IR dipoles	24
18 cm IR dipoles	12

The 8cm dipoles, quadrupoles, and sextupoles were all produced industrially. The low-current correctors, final-focus triplet quadrupoles and beam splitting dipoles were produced internally by BNL. BNL also performed the integration of the quadrupoles, sextupoles, and correctors into a single cryogenic module. The dipole magnets, produced by the Northrop-Grumman Corporation in a build-to-print contract, were complete cryogenic elements suitable for immediate installation.

The crucial aspects of superconducting accelerator magnets are field quality and quench threshold [4]. Since it was decided that cold testing of each magnet was not realistic, field quality was measured at room temperature. It therefore became important to establish a good correlation between warm and cold magnetic field measurements at the 10^{-5} level. An analysis of the complete data set demonstrated that after compensating for yoke saturation effects, good warm/cold field correlations could be obtained at this accuracy. Figure 5 shows a plot of the fractional field deviation on the mid-plane as a function of position.

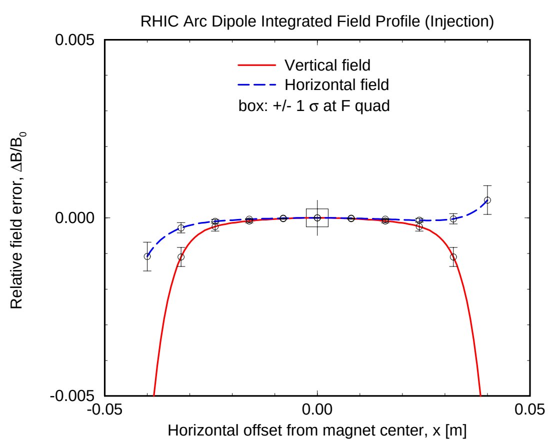

Figure 5: Arc dipole field variation at injection

The magnet set demonstrates excellent field quality with very small random multipole field components by virtue of tight mechanical tolerances on the cable dimensions [5]. The systematic component of the field harmonics is optimized for low-field performance at injection with yoke saturation apparent in the allowed harmonics at high field. During collisions the dynamic aperture is determined by the triplet quadrupoles. The quench performance of the 8 cm dipole magnets is shown in Fig. 6 with the minimum and plateau quench currents for a set of 60 magnets.

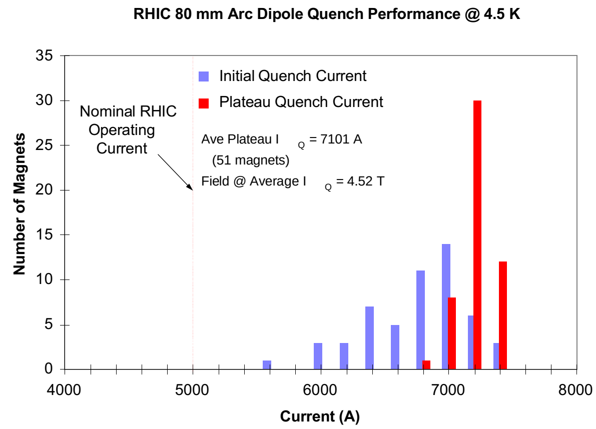

Figure 6: Arc dipole quench performance

Since only 20% of the magnets are measured cold, it is important to demonstrate sufficient operating margin to make limited testing viable. None of the magnets tested to date have had an initial quench current less than the nominal operating level. The plateau quench level demonstrates a healthy 30% operating margin. For the IR magnets however the situation was not so pristine. The large aperture dipole magnets did indeed have an initial quench threshold below the nominal operating point of 6KA. The plateau level on these elements has only a ~10% operating margin and did show some loss of training on a thermal cycle. The data on these magnets is shown in Fig 7.

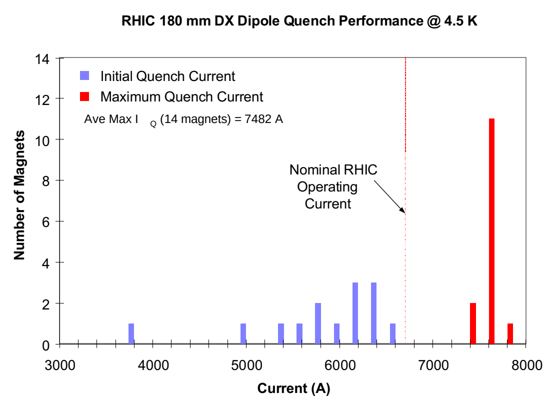

Figure 7: Beam separation dipoles quench performance

5 COMMISSIONING STATUS

The final magnet was delivered to the ring in November 1998. At this point mechanical installation was completed in the arc regions and activities were confined to the beam separation and final focus regions. Installation of the interaction regions was completed two months after the last magnet delivery. Each magnet interconnect requires 20 welded connections and while a local vacuum leak check was performed as part of the installation the necessary leak check sensitivity to ensure an acceptable vacuum at cryogenic temperatures can only be performed when the cryostat is closed up and an insulating vacuum can be established in the cryostat. Leak checking of the system at both low and high pressures in all five cryogenic circuits together with the associated repair took over 10 weeks to complete. With in excess of 25,000 welded joints in the installation process we were pleased to find that we experienced a relatively small number (~25) of helium leaks from the internal piping to the insulating vacuum. Locating and repairing these leaks proved to be relatively slow going since access had to be made through the external cryostat before the repair could be made. In addition, the final focus assembly is mechanically quite complex and precisely locating very small leaks proved difficult on occasion. Another factor that proved to be significant was large leaks masking smaller ones. The machine vacuum was finally certified 'ready-to-go' by the end of March 99 after a few false starts. The main refrigerator was then brought on-line and a purification of the helium circuits was done with a pump/purge cycle. At the time of this conference the cooldown process is just starting. The schedule calls for the rings to be cooled to 50K (the shield temperature) for some helium spill tests and then cryogenic temperatures by the end of April. The first beam tests are scheduled for the end of May after the power supply and quench protection systems are commissioned. We then plan for beam commissioning to continue for two months until the end of July. We goal for this initial operation is to demonstrate collisions of gold ions. The machine will then have a three month summer shutdown when detector equipment will be installed and the first full running period of 37 weeks will start in November 1999. The goals for this run are 10% of design luminosity and 50% up time.

6 REFERENCES

[1] J. Wei, The Evolution of Hadron Beams under Intrabeam Scattering, Proc. 1993 PAC, p. 3653.

[2] J. Wei, Error Compensation in Insertion Region Magnets, Particle Accelerators, 55, p. 439-448, (1996).

[3] S. Peggs, S. Tepikian, D. Trbojevic, A First Order Transition Jump at RHIC, Proc. 1993 PAC, p. 168.

[4] J. Wei, et. al., Field Quality Evaluation of the Superconducting Magnets for the Relativistic Heavy Ion Collider, Proc. 1995 PAC, p. 461.

[5] R. Gupta, Estimating and Adjusting Field Quality in Superconducting Magnets, Particle Accelerators, 55, p. 375, 1996.

ACKNOWLEDGMENTS

The work was performed under the auspices of the U.S. Department of Energy. The author would like to thank Jie Wei, Steve Peggs, Peter Wanderer and Erich Willen, for useful discussions and supplying data for this status report.